Oncolytic avian reovirus-sensitized tumor infiltrating $CD8^+$ T cells triggering immunogenic apoptosis in gastric cancer

Yi-Ying Wu[1,2], Feng-Hsu Wu[3, 4, 5], I-Chun Chen[1,6], Tsai-Ling Liao[7, 8, 9], Muhammad Munir[10], Hung-Jen Liu [1, 2, 8, 9, 11*]

[1]Institute of Molecular Biology, National Chung Hsing University, Taichung, Taiwan

[2]The iEGG and Animal Biotechnology Center, National Chung Hsing University, Taichung, Taiwan

[3]Department of Critical Care, Taichung Veterans General Hospital, Taichung, Taiwan

[4]Division of General Surgery, Department of Surgery, Taichung Veterans General Hospital, Taiwan

[5]Department of Nursing, Hung Kuang University, Taichung, Taiwan

[6]Department of Psychiatry, Taichung Veterans General Hospital, Taichung, Taiwan

[7]Department of Medical Research, Taichung Veterans General Hospital, Taichung, Taiwan

[8]Rong Hsing Research Center for Translational Medicine, National Chung Hsing University, Taichung, Taiwan

[9]Ph.D Program in translational Medicine, National Chung Hsing University, Taichung, Taiwan

[10]Division of Biomedical and Life Sciences, Faculty of Health and Medicine, Lancaster University, Lancaster LA1 4YW, UK

[11]Department of Life Sciences, National Chung Hsing University, Taichung, Taiwan

*To whom correspondence should be addressed: Hung-Jen Liu, Institute of Molecular Biology, National Chung Hsing University, Taichung 402, Taiwan. Phone: 886-4-22840485 ext. 243; Fax: 886-4-22874879; e-mail address: hjliu5257@nchu.edu.tw.

Abstract

This study conducted a comprehensive study to reveal whether oncolytic avian reovirus (ARV)- or UV-inactivated ARV (UV-ARV)-modulated patient peripheral blood mononuclear cells (P-PBMCs) and tumor infiltrating lymphocytes (TILs) killing ARV- and UV-ARV-sensitized adenocarcinoma gastric cell line and primary gastric cancer (PGC) cells derived from gastric cancer of clinical patients. An *in vitro* co-culture model was established to study the interplay between ARV- and UV-ARV-sensitized P-PBMCs and TILs to kill PGC cells. Increased levels of DR4 and DR5 through the TLR3/p38/p53 pathway were observed in ARV and UV-ARV sensitized PGC cells. Importantly, we found that the ARV or UV-ARV σC interact with the surface TLR3 of P-PBMCs and $CD8^+$ TILs, thereby triggering the TLR3/NF-κB/IFN-γ/TRAIL signaling which induces immunogenic apoptosis of PGC cells. This work provides a novel insight into oncolytic ARV and UV-ARV-sensitized P-PBMCs and TILs killing PGC cells through ARV σC-triggering TLR3 receptor and the TRAIL/DR4/DR5 immunogenic apoptosis pathway.

Keywords: apoptosis, cell death, gastric cancer, immune response, signal transduction

Introduction

Oncolytic viruses (OVs) are described as genetically engineered or naturally

45 occurring viruses that specifically replicate and kill cancer cells without affecting
46 normal and healthy cells.[1] OVs including avian reovirus (ARV) are oncolytic viruses
47 that has been extensively studied and applied an oncolytic agent.[2-4] ARVs are not
48 associated with human disease, and pre-existing immunity does not preclude its clinical
49 application.[5,6] The S1 genome segment of ARV contains three open reading frames that
50 are translated into p10, p17, and σC proteins[7], respectively. The oncolytic potential of
51 ARV was originally thought to be attributed mainly to apoptosis[8-10] and ARV σC is
52 known to be an apoptosis inducer capable of inducing apoptosis in Vero and DF-1 cells
53 through p53 and mitochondria-mediated pathways.[9] The p10 protein of ARV can induce
54 syncytia to facilitate virus spread and distribution within a tumor[8], whereas p17 protein
55 induces autophagy, cell cycle arrest, and host cellular translation shutoff and mediates
56 viral protein synthesis and virus replication.[3,5,7] A recent report revealed that p17 protein
57 of ARV induces cell cycle retardation in several cancer cell lines and reduces tumor
58 size *in vivo*.[3]

59 Cytokine-mediated interactions between immune cells and cancer cells are
60 known to affect various aspects of the tumor microenvironment (TME).[11] OVs initiate
61 targeted infection and lysis of tumors while expressing therapeutic transgenes such as
62 cytokines, tumor antigens, checkpoint inhibitors in tumors.[12] TLRs and innate immune
63 response pathways initiate pro-inflammatory cascades, culminating in stimulate

cytokine production that alter the balance of suppressive and activating immune cells.[12,13] In response to inflammatory cytokines, TRAIL is secreted, which binds to the surface DR and triggers caspase 3 activation.[14] TRAIL is one of several TNF family members capable of inducing apoptosis through interaction with DR4 and DR5.[14] ARV-induced cell death may be related to the phenotype of target cells and surrounding TME. PBMCs are blood cells that are an important part of the immune system. They contain a variety of different innate and adaptive cell types.[15,16] PBMCs in the TME belong to the innate (macrophage/monocyte and NK cells) and adaptive (T and B cells) immune system, and their infiltration of tumors (also called TILs) is highly dependent on the presence of soluble factors in the TME.[15,16] Although *in vitro* and *in vivo* studies suggest that OVs may possess high levels of oncolytic activity[15], potential immunogenicity of ARV is poorly understood. None of studies have directly investigated TRAIL expression on PBMCs and TILs that include the innate and adaptive cellular immune response to oncolytic ARV or UV-ARV. The current study provides a novel insight into oncolytic ARV and UV-ARV-sensitized P-PBMCs and TILs killing PGC cells through the TRAIL/DR4/DR5 immunogenic apoptosis pathway.

Results

ARV-induced apoptosis by TRAIL in AGS cells and PGC cells derived from

clinical patients

In this work, virus titers and the levels of DR4, DR5, TLR3, and cytokines were analyzed in ARV-infected AGS cells (online study details of supplementary figures 1-2). To investigate whether TRAIL is involved in ARV-induced AGS cell apoptosis, ARV-induced AGS cell apoptosis by TRAIL was examined. For this purpose, AGS cells were infected with ARV at an MOI of 10 for 24 h, followed by analysis of sub-G1 population by flow cytometry. Importantly, in the presence of TRAIL, ARV significantly enhanced the percentage of sub-G1 population (from 3.9 ± 0.6% to 67.4 ± 7.2%), accompanied by the increased levels of cleaved caspase 3 which was detected by Western blotting (figure 1C) while TRAIL alone only increased to 11.2±1.6% percentage (figure 1A and 1B). Annexin V and PI double staining were also used to examine ARV-induced AGS cell apoptosis. The flow cytometry data was plotted in two-dimensional dot plots where PI represented versus annexin V-FITC. Apoptotic cells which are PI and annexin double positive (PI/FITC +/+) were shown in figure 1D. These findings demonstrate that ARV induces AGS cell apoptosis through the TRAIL/DR4/DR5 apoptotic pathway. Thus, we next intended to examine TRAIL expression in human PBMCs after ARV sensitization. TRAIL levels were analyzed in PBMCs incubated with ARV for 24 hours and found that ARV upregulated expression levels of TRAIL in PBMCs (figure 1E and 1F). Therefore, PBMCs were examined by

two-color flow cytometry 24 hours post ARV sensitization. A significant increase in TRAIL levels was observed post-sensitization in all four major PBMCs populations. Importantly, we found that higher expression levels of TRAIL were observed in $CD3^+$ cells (figure 1G). We next confirmed whether UV-ARV can trigger TRAIL expression in PBMCs. For this purpose, the TRAIL expressions of $CD56^+$, $CD14^+$, $CD3^+$ and $CD19^+$ were examined by two-color flow cytometry 24h after UV-ARV incubation. Interestingly, it was observed that stimulation with UV-ARV was sufficient to induce TRAIL expression on PBMCs (figure 1G). Taken together**,** our findings revealed that TRAIL expression is not dependent on direct infection of the TRAIL-expressing cells (figure 1G).

Our findings that ARV-induced apoptosis by TRAIL in AGS cells but not PBMCs are shown in the study details of supplementary information (online study details of supplementary figures 3-5). Thus, we next wanted to study whether the same effect is also achieved on the PGC cells and P-PBMCs of gastric cancer patients. In this study, normal patient epithelial cells and PGC cells were characterized by the detection of cytokeratin 18 antigen and GRN markers, respectively (figure 2A and B)**.** Next, sub-G1 populations were analyzed by flow cytometry where PGC cells were infected with ARV with an MOI of 10 for 24 hours. In the presence of TRAIL, ARV significantly enhanced the percentage of sub-G1 populations, while TRAIL alone only slightly

induced apoptosis (figure 2C and D). These results suggest that ARVs induce apoptosis in PGC cells through the TRAIL apoptotic signaling. ARV-sensitized P-PBMCs can selectively and efficiently kill malignant PGC cells sparing normal counterparts (figure 2C and D). Annexin V and PI double staining were used to examine ARV-induced apoptosis in PGC cells. The data generated by flow cytometry was plotted in two-dimensional dot plots and analysis indicated that apoptotic cells were PI and annexin double positive (PI/FITC+/+) (figure 2E). P-PBMCs were isolated from volunteers of GC patients.

ARV and UV-ARV- sensitized TRAIL expression on GC patient's PBMCs

TRAIL levels were analyzed in P-PBMCs sensitized with ARV for 24 h. P-PBMCs were examined by two-color flow cytometry 24 h post ARV sensitization. When sensitized, a significant TRAIL levels were observed in all four major P-PBMC populations (figure 2F). We found that highest expression levels of TRAIL were observed in patient's $CD3^+$ T cell (figure 2F). We next wanted to confirm whether UV-ARV can trigger TRAIL expression of P-PBMCs. Thus, $CD56^+$, $CD14^+$, $CD3^+$, and $CD19^+$ were examined by two-color flow cytometry for TRAIL expression 24 h after UV-ARV sensitization. Interestingly, sensitization with UV-ARV was sufficient to induce TRAIL expression on P-PBMC populations (figure 2F). Taken together, our results revealed that TRAIL

140 expression is independent of direct infection.

141

142 **TRAIL upregulation dependent on IFN-γ sensitization but not direct infection and**

143 **IFN-γ driven expression of TRAIL on P-PBMCs**

144 Our analysis of IFN-γ levels in ARV-sensitized P-PBMCs revealed that ARV-sensitized

145 P-PBMCs produce high levels of IFN-γ (figure 3A). A similar trend was also observed

146 in UV-ARV-sensitized P-PBMCs (figure 3A). Furthermore, intracellular staining of

147 IFN-γ revealed that $CD3^+$ and $CD56^+$ cells produced a high level of IFN-γ cytokine

148 after ARV sensitization (figure 3A). To verify that TRAIL expression was driven by

149 IFN-γ, the expression levels of TRAIL in ARV-sensitized cells in the presence of anti-

150 IFN-γ neutralizing antibodies or medium alone were analyzed. The increased levels of

151 TRAIL in $CD3^+$ and $CD56^+$ cells were observed in ARV-sensitized P-PBMCs. This

152 effect was reversed in cells-treated with the IFN-γ antibody (figure 3B). Taken together,

153 the results demonstrate that increased levels of TRAIL on ARV-sensitized P-PBMCs

154 are regulated by the IFN-γ signaling. To investigate whether ARV or UV-ARV

155 sensitizes IFN-γ of P-PBMCs, the ARV or UV-ARV-sensitized P-PBMCs were divided

156 into cultures with decreased cell numbers. As expected, decreased numbers of P-

157 PBMCs accompanied by decreased levels of IFN-γ in the cultures (figure 3C). These

158 finding demonstrates that increased levels of TRAIL on ARV-sensitized or UV-ARV-

159 sensitized P-PBMCs are regulated by IFN-γ signaling.

160

161 **ARV or UV-ARV-sensitized GC patient's PBMCs killing ARV-infected or UV-**

162 **ARV sensitized PGC cells**

163 To investigate whether sensitization of P-PBMCs kill PGC cells, we examined

164 responsiveness of PGC cells co-cultured with P-PBMCs after ARV or UV-ARV

165 sensitization. ARV-unsensitized P-PBMCs induces minimal apoptosis of PGC cells,

166 whereas ARV or UV-ARV-sensitized P-PBMCs induced strong apoptosis of PGC cells

167 (figure 4A-B). To confirm whether ARV-modulated cytotoxic activity of P-PBMCs is

168 TRAIL-dependent, PGC cells co-cultured with P-PBMCs were treated with either

169 DR5:Fc or Fas:Fc prior to their sensitization with ARV or UV-ARV. Under these

170 conditions, DR5:Fc reversed apoptosis of PGC cells, whereas no change was observed

171 in ARV-sensitized P-PBMCs treated with Fas:Fc (figure 4A-B). Similar results were

172 observed in UV-ARV-sensitized P-PBMCs (figure 4A-B), indicating that infection is

173 not required to induce TRAIL expression in P-PBMCs. UV-ARV potently activate P-

174 PBMCs to induce apoptosis of PGC cells (figure 4A-B). Furthermore, the cytotoxic

175 effect on PGC cells was assessed by an LDH release assay. As shown in figure 4C, after

176 sensitization with ARV or UV-ARV, $CD3^+$ cells displayed a strong cell killing activity

177 on PGC cells.

ARV or UV-ARV-sensitized $CD8^+$ TILs but not $CD4^+$ TILs killing PGC cells

We found that gastric TILs are composed of $CD4^+$ and $CD8^+$ (about 75%), $CD14^+$ (<10%), and $CD56^+$ (<5%) infiltrating the gastric tumor together. Compared with $CD8^+$ TILs, $CD4^+$ TILs were more efficient at host immune activation but less capable of direct tumor killing. Since $CD8^+$ TILs maintain high cytotoxicity, cytotoxic activity on PGC cells was assessed by LDH release assay. As shown in figure 5A, $CD8^+$ TILs display a strong cell killing activity on PGC cells when sensitized with ARV (10 MOI) or UV-ARV (10 and 100 MOIs). Treatment of $CD8^+$TILs with ARV (10 MOI) or UV-ARV at various MOIs (10-100) could not induce apoptosis in $CD8^+$TILs (supplementary figure 6). TRAIL expression by $CD8^+$TILs sensitized with ARV or UV-ARV were shown in figure 5B. To further confirm the necessity of IFN-γ to drive TRAIL expression, $CD8^+$ TILs were sensitized with ARV or UV-ARV for 24 h followed by treatments with neutralizing IFN-γ mAb or isotype mAb. Our results revealed that treatment with the neutralizing IFN-γ mAb failed to induce TRAIL expression (Figure 5C), suggesting that TRAIL on ARV or UV-ARV-sensitized TILs is induced by IFN-γ. IFN-γ produced by $CD8^+$ TILs enhanced TRAIL expression was essential to sustaining the cytotoxicity of $CD8^+$ TILs. After treatment of ARV or UV-ARV, we found that the expression level of TRAIL was increased in ARV- or UV-ARV-sensitized $CD8^+$ TILs

thereby enhancing TRAIL-specific killing PGC cells. This is the first report to show direct interaction between $CD8^+$TILs and PGC cells regulated by ARV and UV-ARV in an *in vitro* co-culture system.

ARV- or UV-ARV-sensitized $CD8^+$TILs expressing TRAIL which kills PGC cells

To investigate whether sensitization of $CD8^+$ TILs directly kill PGC cells in TME, we examined responsiveness of PGC cells co-cultured with $CD8^+$ TILs after different treatments with ARV or UV-ARV. ARV- or UV-ARV-unsensitized $CD8^+$ TILs induced minimal apoptosis of PGC cells, whereas ARV or UV-ARV-sensitized $CD8^+$ TILs induced strong apoptosis of PGC cells. To further confirm whether ARV- or UV-ARV-modulated cytotoxic activity of $CD8^+$ TILs is through a TRAIL-dependent manner, PGC cells co-cultured with $CD8^+$ TILs were treated with either DR5:Fc or Fas:Fc prior to their sensitization with ARV or UV-ARV (figure 6A-C). Under these conditions, DR5:Fc reversed apoptosis of PGC cells, while no change was observed in UV-ARV or ARV-sensitized $CD8^+$ TILs treated with Fas:Fc (figure 6A-C). Similar results were observed in UV-ARV-sensitized $CD8^+$ TILs (figure 6A-C), indicating that ARV infection is not required to induce TRAIL expression in $CD8^+$ TILs. Our study documented that ARV- and UV-ARV-sensitized $CD8^+$ TILs killing PGC cells was mainly mediated by IFN-γ and TRAIL. *In vitro* co-cultures revealed that killing of PGC

cells were enhanced by ARV- or UV-ARV-sensitized $CD8^+$ TILs.

ARV or UV-ARV-sensitized $CD8^+$ TILs induces the IFN-γ expression through the TLR3/NF-κB signaling pathway

A previous study suggested that human effector $CD8^+$ cells express TLR3 as a functional coreceptor.[17] To determine whether ARV or UV-ARV σC protein interacts with cell surface TLR3 on $CD8^+$ TILs, interactions between σC protein with cell surface TLR3 of $CD8^+$ TILs were analyzed by *in situ* PLA. Tumor infiltrating cytotoxic T-cells carry higher nuclear to cytoplasmic ratios[18] and oncolytic viruses specifically replicate and infect cancer cells without affecting healthy cells including $CD8^+$ TILs.[1,15] Our results clearly indicated that σC protein interacts with cell surface TLR3 of $CD8^+$ TILs (figure 7A). In contrast, no signal was observed in negative controls (figure 7A). Previous study had indicated that TLR3-induced signaling spreads to several adaptors and downstream activation of NF-κB.[17] These prompted us to investigate whether ARV or UV-ARV induces $CD8^+$ TILs expressing IFN-γ through the TLR3/NF-κB signaling pathway. In this work, $CD8^+$ TILs were treated with the TLR3 inhibitor followed sensitization with ARV or UV-ARV. The results in Figure 7B-C showed that the TLR3 inhibitor significantly decrease the expression levels of IFN-γ in ARV or UV-ARV-sensitized $CD8^+$ TILs. Having shown that ARV or UV-ARV could induce $CD8^+$ TILs

235 secretion of IFN-γ (Figure 7B-C), we next wanted to examine whether the upstream
236 signaling of IFN-γ. NF-κB is an inducible transcription factor that is involved in the
237 cytokine-induced immune response.[13,17] As shown in Figure 7B-C, treatment with the
238 NF-κB inhibitor resulted in reduced expression of IFN-γ in ARV or UV-ARV
239 sensitized-$CD8^+$TILs, suggesting that UV-ARV or ARV induced $CD8^+$TILs secretion
240 of IFN-γ through the NF-κB signaling pathway. Taken together our results suggested
241 that ARV or UV-ARV-induced IFN-γ secretion of $CD8^+$ TILs is dependent on σC-
242 triggering the TLR3/NF-κB/IFN-γ/TRAIL immunogenic apoptosis pathway.
243
244 **Upregulation of the DR4 and DR5 expression through the p38/p53 signaling**
245 **pathway in ARV or UV-ARV-sensitized PGC cells**
246 Our results indicated that ARV or UV-ARV treatments upregulates DR4 and DR5
247 expression on PGC cells by flow cytometry (Figure 8A). Since DR4 and DR5 are
248 transmembrane domains and cytoplasmic domains of TRAIL receptors[19], which are
249 upregulated on PGC cell surface by ARV or UV-ARV, this directed us to further confirm
250 whether ARV-induced apoptosis of PGC cells occurs due to host signal transduction
251 pathway. Our previous study indicated that σC induces apoptosis in cultured cells and
252 activates a proapoptotic signal by linking p38 to p53.[20] We next wanted to elucidate
253 whether the p38/p53 signaling pathway upregulates the expression of DR4 and DR5.

In this work, PGC cells were pre-treated with the p53 inhibitor for 5 h followed by treatments with ARV or UV-ARV. The results shown in Figure 8A indicated that the p53 inhibitor significantly decreased the expression levels of DR4 and DR5 in ARV or UV-ARV-sensitized PGC cells. Furthermore, our results revealed that inhibition of p38 by the inhibitor significantly decreased the expression levels of p53 and p-p53 (S15) in ARV or UV-ARV-sensitized PGC cells (Figure 8B). Treatment with the TLR3 inhibitor reduced the phosphorylated form of p-p38 (T180) in ARV or UV-ARV sensitized-PGC cells, suggesting that UV-ARV or ARV upregulates DR4 and DR5 expression on PGC cells through the p38/p53 signaling pathway (Figure 8C).

Surface expression of TLR3 has been reported in various cancers and TLR3 occur both in the cell membrane and intracellularly, and it seems that activation of the immune response can be initiated concurrently from these two sites in the cell.[21] To study the upstream signaling, we investigated whether ARV or UV-ARV σC protein interacts with the surface TLR3 on PGC cells. Interactions between σC protein with the surface TLR3 of PGC cells were analyzed by *in situ* PLA. Our results revealed that σC protein interacts with TLR3 of PGC cells (Figure 8D). In contrast, no signal was observed (Figure 8D). Our previous study suggested that cell entry of avian reovirus follows a caveolin-1-mediated and dynamin-2-dependent endocytic pathway that requires activation of p38 signaling pathway[22] and cancer cell entry of ARV modulated by σC

binging to cell receptors triggers endocytosis.[23] Our results for the first time suggested that ARV or UV-ARV-induced DR4 and DR5 expression of PGC cells is dependent on σC-triggering the TLR3/p38/p53/DR4/DR5 pathway.

Discussion

A perfect OV should eliminate cancer cells through a combination of three mechanisms: including induction of apoptosis, pro-inflammatory cytokines, and IFNs.[24,25] Besides directly kill tumor cells, OV can activate immune responses or express healing factors to increase antitumor efficacy and enhances efficacy of cancer immune oncological therapy.[26,27] OV-mediated apoptosis may trigger anticancer immune responses in TEM.[28] Modulation of apoptosis is beginning as a new immunotherapeutic approach for the treatment of cancer.[29] The novel discovery that oncolytic ARV-modulated upregulation of the TLR3/NF-kB/IFN-γ/TRAIL pathway in $CD8^+$TILs, triggering PGC cells of apoptosis through the TLR3/p38/p53/DR4/DR5 pathway.

Previous studies suggested that IFN-γ mediates apoptosis of kidney tubular epithelial cells[30] and induces apoptosis through the Jak/Stat pathway by the type I IFN receptor in human colon cancer cells.[31] Although the innate antiviral system of cancer cells may be resistant to the treatment of oncolytic ARV, interestingly, IFN-γ does not

292 inhibit ARV-induced TRAIL expression and ARV-modulated TRAIL-induced apoptosis,
293 suggesting that ARV-induced apoptosis was more sensitive to the TRAIL. Our finding
294 is supported by a previous report suggesting that TRAIL has been implicated in having
295 the IFN-γ response promotor.[32] This study provides a mechanistic insight into ARV- or
296 UV-ARV-sensitized $CD8^+$ TILs expressing TRAIL through activation of the TLR3/NF-
297 kB/IFN-γ pathway preferentially killing PGC cells by immunogenic apoptosis. A model
298 illustrating ARV and UV-ARV-sensitized $CD8^+$ TILs killing PGC cells is outlined in
299 figure 9.

300 The use of OV to treat cancer either directly kill OV-infected tumor cells or
301 increase their susceptibility to cell death or apoptosis.[33] A previous study provides
302 potential strategies in cancer treatments with OV and adjuvant NK cells in a cancer
303 treatment.[34] It was reported that TRAIL-armed oncolytic poxvirus suppresses lung
304 cancer cells by inducing apoptosis.[35] Lal et. al. developed recombinant measles virus
305 armed with BNiP3 (a pro-apoptotic gene of human origin) as an oncolytic agent to
306 induce apoptosis in breast cancer cells *in vitro*.[36] Importantly, our findings reveal that
307 oncolytic ARV could be an effective therapeutic strategy for treatment of gastric cancers.
308 This study provides a better insight into *in vitro* mechanistic immunological studies
309 bridging a systemic model and possibly enable the development of ARV targeted
310 immunomodulatory therapies.

311 Multiple signaling pathways commonly involved in viral clearance, including
312 IFNs, TLRs, and double-stranded RNA-activating protein kinase (PKR) pathways, may
313 be defective or inhibited in cancer cells, allowing OV to enter and survive in these
314 cells.[12,37] We have demonstrated for the first time that UV-ARV and ARV σC protein
315 interacts with surface TLR3 of $CD8^+$ TILs and PGC cells. Interestingly, our *in situ* PLA
316 revealed different staining phenotypes between $CD8^+$ TILs and PGC cells. Oncolytic
317 ARV can exclusively replicate and infect cancer cells (PGC cells), but it is unable to
318 infect healthy cells ($CD8^+$ TILs).[4,38] We have demonstrated that ARV infects Vero, DF-
319 1 and AGS cancer lines through σC binding to cellular receptors[23], thereby triggering
320 cavolin and dynamin 2-dependent endocytosis and signaling activation[22,23] Our
321 previous observation supported that interaction of ARV σC protein with cell surface
322 TLR3 only in $CD8^+$TIL but evenly distributed of the PGC cells.
323 MRV displays tropism and efficiently replicates in tumor cells with the activated
324 Ras pathway.[39] These characteristics allow the use of MRV in virotherapy, either alone
325 or combined with the conventional and nonconventional treatments.[33,39] For instance,
326 synergistic cytotoxicity of MRV in combination with cisplatin-paclitaxel doublet
327 chemotherapy.[39] Currently, REOLYSIN®, a formulation of MRV, is used in cancer
328 therapeutics, which has been tested at the preclinical stage and phases I-III clinical
329 studies in a broad range of cancer indications.[39] Our evidences suggest that the

antitumoral mechanism associated with ARV or UV-ARV involves the activation of immune response to immunogenic apoptosis. ARV or UV-ARV optimized to attract immune cells to express TRAIL might favorably change the TME. Furthermore, reactive expression of TRAIL in the TME could be a mechanism of resistance to cancer, which induced by IFN-γ. Recent evidence suggests that NK cells can recognize viruses themselves, as in the case of cytomegalovirus which promotes the generation of memory-like NK cells in humans and have an increased IFN-γ and cytolytic response on encounter with target cells.[40] In this study, treatments of PGC cells with ARV and UV-ARV induced a systemic antitumor $CD8^+$ cells response, prominent infiltration of cytotoxic T lymphocytes and Th1 type polarization. Th1 cells produce cytokines, particularly IFN-γ, which play a role in activation and enhancement of cytotoxic T cell expansion and effector functions.[38,41] Although activated cytotoxic T cells are present in many human tumors, but tumors fail to undergo spontaneous regression.[11,17] $CD8^+$TILs were found to have an altered phenotype and an impaired ability to secrete IFN-γ. Importantly, oncolytic ARVs or UV-ARVs exert a regulatory role to enhance response of $CD8^+$TILs in the TME. This study demonstrates ARV- or UV-ARV-modulated direct interaction between TILs and PGC cells in an *in vitro* co-culture system. In our co-culture model, ARV or UV-ARV virotherapy induced a strong $CD8^+$TILs immunity that is therapeutically effective against PGC cells. These support

the preclinical development of ARV and UV-ARV as an adjuvant to treat human gastric cancer. This study sheds further light on the molecular basis behind ARV and UV-ARV and facilitates the future efficacy of ARV and UV-ARV as a cancer therapeutic.

Materials and Methods

Virus and cell line

The S1133 strain of ARV was used in this study. Human adenocarcinoma gastric cell line (AGS) was cultured in Dulbecco's Modified Eagle's Medium (DMEM) (Biochrom co, Berlin, Germany) supplemented with 10% fetal bovine serum (FBS), 1% penicillin/streptomycin, and 10 mM 4-(2-hydroxyethyl) piperazine-1-ethanesulphonic acid (HEPES) (pH 7. 2) at 37°C in a 5% CO_2 incubator.

Ethical standards and human samples

Ex vivo normal and malignant gastric tissues were obtained from patients undergoing routine planned cancer-related surgery. Written informed consent was obtained from each patient in accordance with local institutional ethics review and has been approved by the Ethical and Scientific Committee of Taichung Veterans General Hospital (TCVGH-IRB no. SF22141B#1). Clinical characteristics of patient's samples used in this study are shown in Table 1. All patients have a history of gastric cancer without

chemotherapy. The absence of *H. pylori* infection was confirmed using histological examination. Histological examination of gastric biopsies was obtained from upper gastrointestinal endoscopy which were carried out in all ascertainment of gastric cancer cases.

Human primary gastric cell culture from fresh surgical gastric tissues

The specimens are collected in Dulbecco's modified Eagle's medium (DMEM) (Biochrom Co, Berlin, Germany) containing 1% Penicillin/Streptomycin for transport to our laboratory. Cell culture of primary human gastric cancer cells and gastric normal epithelial cells were purified and maintained in DMEM medium supplemented with 10% FBS as previously described.[42,43] On the next day, cell culture was rinsed with PBS twice to remove non-adherent cells. The medium was changed every 3-7 days, depending on the density of cell growth. The colonies increase in size and spread out, resulting in some cells separating at the periphery of the colonies after 2 weeks of culture. Gastric normal epithelial cells were confirmed by flow cytometry analysis of cytokeratin 18 (CK-18) expression. Primary GC cells were identified using granulin (GRN) markers.[42] These primary cells were maintained in culture for up to 4-8 weeks.

Sorting of T cells, B cells, monocytes/macrophages, NK Cells and PGC cells

PBMCs were stained with the CD3 Ab for T cells, CD56 Ab for NK cells, CD19 Ab for B cells, CD14 Ab for monocyte/macrophage cells. TILs were stained with CD8 Ab for cytotoxic T cells (CTLs), CD4 Ab for helper T cells (Th cells), CD56 Ab for NK cells, and CD14 Ab for monocyte/macrophage cells. Gastric normal epithelial cells were stained with CK-18. PGC cells were stained with GRN. Sample acquisition and cell sorting was managed on the BD FACSMelody™ cell sorter (BD Biosciences, San Jose, USA) and BD Chorus software (BD Biosciences, San Jose, CA). All antibodies used in this study are shown in supplementary Table 1.

Isolation of TILs

The generation of TIL cultures by tumor has been described in detail.[44] Briefly, the tumor removed from cancer patients was placed on a plate with 5% FBS in Hank's Balanced Salt Solution (HBSS) buffer (Gibco, New York, USA) on ice and disintegrated using scissors. The homogenate was collected and treated with 1 mg/ml type IV collagenase (Sigma, St. Louis, USA) and 0.05 mg/ml DNase (Promega, Madison, USA) for 30 minutes at 37°C with gentle agitation. The digested extract was screened using a 100-mesh, and the filtrate was washed with 5% FBS in HBSS buffer and centrifuged at 600xg for 7 minutes at 4°C. The cell pellet obtained was treated with ACK erythrocyte lysis buffer (155 mM NH_4Cl, 10 mM $KHCO_3$, and 1 mM Na_2EDTA,

406 pH 7.3) for 5 min at room temperature. Finally, TILs were resuspended in RPMI 1640
407 medium with 10% FBS. Cells were harvested by 7 to 14 days of culture. Each initial
408 well was considered to be an independent TIL culture and maintained separately from
409 the others.
410
411 **Co-culturing of immune cells and cancer cells in presence of ARV or UV-ARV**
412 The ratio of PBMCs (effector cells) to AGS cells (cancer cell lines) is 5:1. The selected
413 ratio is according to a previous report by Doumba.[45] For direct *in vitro* co-culture, PGC
414 cells were plated with p-PBMCs or TILs from the same patient at a 1:5 ratio in reduced-
415 serum medium (2% FBS). The selected ratio is based on AGS cells and PBMCs. The
416 cultures were incubated for 3 days, after which cells were sensitized with the ARV or
417 UV-ARV for 24 h and 48 h.
418
419 **Detection of cytotoxicity of PBMCs and TILs**
420 The cytotoxicity of PBMCs and TILs were estimated by quantification of LDH activity
421 in the culture medium by using the QuantiChrom^{TM} LDH Cytotoxicity Assay Kit
422 (BioAssay Systems, Hayward, USA).[46,47] Briefly, cytotoxicity assays were carried out
423 in 96-well plates with a final sample volume of 100 µl/well. Target cells (AGS cells and
424 PGC cells, 2×10^5/ml cells) in 50 µl/well were co-cultured with effector cells (normal

PBMCs, patient's PBMCs, and TILs) at various effector to target ratios (5:1) for 4h.[20]

Phosphoprotein staining[48]

Phosphoproteins were measured in either unstimulated PGC cells or stimulated with ARV or UV-ARV for 24 hours in the presence or absence of inhibitors. For anti-p38, anti-phospho-p38, anti-p53 and anti-phospho-p53 antibody detection, the intracellular staining was performed using Fixation/Permeabilization Solution Kit (Cytofix/Cytoperm BD Biosciences, San Jose, USA), according to the manufacturer's instructions. Data were collected with a FACSCANTO II multicolor flow cytometer and analyzed.

Statistical analysis

Statistical analyses and figures were generated using GraphPad Prism 8.0 software (GraphPad Software Inc., La Jolla, USA). Differences between means were evaluated using the Student's *t-test* and were deemed significant at $*p \leq 0.05$ and $**p \leq 0.01$.

Acknowledgements

This work was supported by grants from Ministry of Science and Technology of Taiwan (112-2313-B-005-050-MY3), The iEGG and Animal Biotechnology Center

from The Feature Areas Research Center Program within the framework of the Higher Education Sprout Project by the Ministry of Education (MOE) in Taiwan (113S0023A), Taichung Veterans General Hospital (TCVGH-NCHU-1137607).

Author contributions All authors made substantive intellectual contributions to the present study and approved the final manuscript. H.J.L. conceived of the study and generated the original hypothesis, wrote the paper, and supervised the project; Y.Y.W. performed most of the experiments. I.C.C., F.H.W., T.L.L., Y.Y.W., and M. M. analyzed data. I.C.C., F.H.W., T.L.L., Y.Y.W. performed statistical analysis. H.J.L., M.M. revised and edited the manuscript.

Competing interest We declare that we have no competing interests.

Patient consent for publication not required.

Ethics approval the protocol was approved by the ethics committee of Hospital

Provenance and peer review not commissioned; externally peer reviewed.

Data availability statement Data are available in a public, open-access repository. All data relevant to the study are included in the article or uploaded as supplementary information.

References

1. Fukuhara, H., Ino, Y. & Todo, T. Oncolytic virus therapy: A new era of cancer

treatment at dawn. *Cancer Sci* **107,** 1373-1379 (2016).

2. Kozak, R.A. et al. Replication and oncolytic activity of an avian orthoreovirus in human hepatocellular carcinoma cells. *Viruses* **9**, 90 (2017).

3. Chiu, H.C. et al. Mechanistic insights into avian reovirus p17-modulated suppression of cell cycle CDK-cyclin complexes and enhancement of p53 and cyclin H interaction. *J. Biol. Chem.* **293,** 12542-12562 (2018).

4. Cai, R. et al. The oncolytic efficacy and safety of avian reovirus and its dynamic distribution in infected mice. *Exp. Biol. Med.* (Maywood) **244**, 983-991 (2019).

5. Chiu, H.C. et al. Heterogeneous nuclear ribonucleoprotein A1 and lamin A/C modulate nucleocytoplasmic shuttling of avian reovirus p17. *J. Virol.* **93**, e00851-19 (2019).

6. De, Carli. S. et al. Genotypic characterization and molecular evolution of avian reovirus in poultry flocks from Brazil. *Avian Pathol.* **49**, 611-620 (2020).

7. Huang, W.R. et al. p17-modulated Hsp90/Cdc37 complex governs oncolytic avian reovirus replication by chaperoning p17, which promotes viral protein synthesis and accumulation of viral proteins σC and σA in viral factories. *J. Virol.* **96**, e0007422 (2022).

8. Liu, H.J. et al. Activation of small GTPases RhoA and Rac1 is required for avian reovirus p10-induced syncytium formation. *Mol. Cells* **26**, 396–403 (2008).

9. Chulu, J.L. et al. Apoptosis induction by avian reovirus through p53 and mitochondria-mediated pathway. *Biochem. Biophys. Res. Commun.* **356**, 529-535 (2007).

10. Lin, P.Y. et al. Avian reovirus S1133-induced DNA damage signaling and subsequent apoptosis in cultured cells and in chickens. *Arch. Virol.* **156**:1917-1929 (2011).

11. Boulch, M. et al. A cross-talk between CAR T cell subsets and the tumor microenvironment is essential for sustained cytotoxic activity. *Sci Immunol.* **6**, eabd4344 (2021).

12. Rommelfanger, D.M. et al. The efficacy versus toxicity profile of combination virotherapy and TLR immunotherapy highlights the danger of administering TLR agonists to oncolytic virus-treated mice. *Mol. Ther.* **21**, 348-357(2013).

13. Furman, D. & Davis, M.M. New approaches to understanding the immune response to vaccination and infection. *Vaccine* **33**, 5271-5281 (2015).

14. Yuan, X. et al. Developing TRAIL/TRAIL death receptor-based cancer therapies. *Cancer Metastasis Rev.* **37**, 733-748 (2018).

15. Kumar, V., Giacomantonio M.A. & Gujar, S. Role of myeloid cells in oncolytic reovirus-based cancer therapy. *Viruses* **13**, 654 (2021).

16. Grievink, H.W. et al. Comparison of three isolation techniques for human peripheral blood mononuclear cells: cell recovery and viability, population composition, and cell functionality. *Biopreserv. Biobank* **14**, 410-415 (2016).

17. Tabiasco J. et al. Human effector CD8+ T lymphocytes express TLR3 as a functional coreceptor. *J. Immunol.* **177**, 8708-8713 (2006).

18. Liu, W.H. et al. Efficient enrichment of hepatic cancer stem-like cells from a primary rat HCC model via a density gradient centrifugation-centered method. *PLoS One* **7**, e35720 (2012).

19. Mérino D. et al. Differential inhibition of TRAIL-mediated DR5-DISC formation by decoy receptors 1 and 2. *Mol. Cell Biol.* **26**, 7046-7055 (2006).

20. Lin, P.Y. et al. Modulation of p53 by mitogen-activated protein kinase pathways and protein kinase C δ during avian reovirus S1133-induced apoptosis. *Virology* **385**, 323-334 (2009).

513 21. Matylda, B.M., Magdalena, B.N. & Felix, N.T. Cell surface expression of
514 endosomal Toll-like receptors-A necessity or a superfluous duplication? *Front.*
515 *Immunol.***11**, 620972 (2021).
516 22. Huang, W.R. et al. Cell entry of avian reovirus follows a caveolin-1-mediated and
517 dynamin-2-dependent endocytic pathway that requires activation of p38
518 mitogen-activated protein kinase (MAPK) and src signaling pathways as well
519 as microtubules and small GTPase rab5 protein. *J. Biol. Chem.* **286**, 30780-
520 30794 (2011).
521 23. Huang, W.R. et al. Cell entry of avian reovirus modulated by cell-surface annexin
522 A2 and adhesion G protein-coupled receptor latrophilin-2 triggers src and p38
523 MAPK signaling enhancing caveolin-1-and dynamin 2-dependent endocytosis.
524 *Microbiol. Spectr.* **11**, e0000923 (2023).
525 24. Mahmoud, M.H. et al. Elevated IFN-alpha/beta levels in a streptozotocin-induced
526 type I diabetic mouse model promote oxidative stress and mediate depletion of
527 spleen-homing $CD8^+$ T cells by apoptosis through impaired CCL21/CCR7 axis
528 and IL-7/CD127 signaling. *Cell Signal* **27**, 2110-119 (2015).
529 25. Frumence, E. et al. The South Pacific epidemic strain of Zika virus replicates
530 efficiently in human epithelial A549 cells leading to IFN-β production and
531 apoptosis induction. *Virology* **493**, 217-226 (2016).
532 26.Yang, C. et al. Oncolytic viruses as a promising therapeutic strategy for
533 hematological malignancies. *Biomed Pharmacother.* **139**, 111573 (2021).
534 27. Sobhanimonfared, F. et al. Virus specific tolerance enhanced efficacy of cancer
535 immuno-virotherapy. *Microb. Pathog.* **140**, 103957 (2020).
536 28. Ma, J. et al. Characterization of virus-mediated immunogenic cancer cell death and
537 the consequences for oncolytic virus-based immunotherapy of cancer. *Cell*

538 *Death Dis.* **11**, 48 (2020).
539 29. Lecoultre, M., Dutoit, V. &Walker, P.R. Phagocytic function of tumor-associated
540 macrophages as a key determinant of tumor progression control: a review. *J.*
541 *Immunother. Cancer.* **8**, e001408 (2020).
542 30. Du, C. et al. IL-2-mediated apoptosis of kidney tubular epithelial cells is regulated
543 by the caspase-8 inhibitor c-FLIP. *Kidney Int* **67**, 1397-1409 (2005).
544 31. Sun, Y. et al. Regulation of XAF1 expression in human colon cancer cell by
545 interferon beta: activation by the transcription regulator STAT1. *Cancer Lett.*
546 **260**, 62-71 (2008).
547 32. Häcker, S. et al. Histone deacetylase inhibitors cooperate with IFN-gamma to
548 restore caspase-8 expression and overcome TRAIL resistance in cancers with
549 silencing of caspase-8. *Oncogene* **28**, 3097-3110 (2009).
550 33. Goldufsky, J. et al. Oncolytic virus therapy for cancer. *Oncolytic Virother.* **2**, 31-46
551 (2013).
552 34. Aspirin, A.P., de Los Reyes, V.A. & Kim, Y. Polytherapeutic strategies with
553 oncolytic virus-bortezomib and adjuvant NK cells in cancer treatment. *J. R. Soc.*
554 *Interface.* **18**, 20200669 (2021).
555 35. Hu, J. et al. Trail armed oncolytic poxvirus suppresses lung cancer cell by inducing
556 apoptosis. *Acta. Biochim. Biophys. Sin.* (Shanghai) **50**,1018-1027 (2018).
557 36. Lal, G. & Rajala, M.S. Combination of oncolytic measles virus armed with BniP3,
558 a pro-apoptotic gene and paclitaxel induces breast cancer cell death. *Front.*
559 *Oncol.* **8**, 676 (2018).
560 37. Heggen-Peay, C.L. et al. Interactions of poult enteritis and mortality syndrome-
561 associated reovirus with various cell types in vitro. *Poult. Sci* 81:1661-1667
562 (2002).

563 38. Wu, Y.Y. et al. Oncolytic viruses-modulated immunogenic cell death, apoptosis and
564 autophagy linking to virotherapy and cancer immune response. *Front Cell Infect*
565 *Microbiol* **13**, 1142172 (2023).
566 39. Roulstone, V. et al. Synergistic cytotoxicity of oncolytic reovirus in combination
567 with cisplatin-paclitaxel doublet chemotherapy. *Gene Ther* **20**, 521-528 (2013).
568 40. Forrest, C. et al. NK cell memory to cytomegalovirus: implications for vaccine
569 development. *Vaccines* (Basel) **8**, 394 (2020).
570 41. Kim, K.B. et al. Potentiation of Fas- and TRAIL-mediated apoptosis by IFN-gamma
571 in A549 lung epithelial cells: enhancement of caspase-8 expression through
572 IFN-response element. *Cytokine* **20**, 283-288 (2002).
573 42. Aziz, F. et al. A method for establishing human primary gastric epithelial cell culture
574 from fresh surgical gastric tissues. *Mol. Med. Rep.* **12**, 2939-2944 (2015).
575 43. Smoot, D.T. et al. A method for establishing primary cultures of human gastric
576 epithelial cells. *Methods Cell Sci* **22**, 133-136 (2000).
577 44. Mark, E.D. et al. Generation of tumor-infiltrating lymphocyte cultures for use in
578 adoptive transfer therapy for melanoma patients. *J. Immunother.* **26**, 332-342
579 (2003).
580 45. Doumba, P.P. et al. Co-culture of primary human tumor hepatocytes from patients
581 with hepatocellular carcinoma with autologous peripheral blood mononuclear
582 cells: study of their in vitro immunological interactions. *BMC*
583 *Gastroenterol.***13**,17 (2013).
584 46. Vergis, J. et al. Exploring galleria mellonella larval model to evaluate antibacterial
585 efficacy of cecropin A (1-7)-melittin against multi-drug resistant
586 enteroaggregative Escherichia coli. *Pathog. Dis.* **79**,ftab010 (2021).
587 47. Zhou, Y. et al. Retrospective analysis of the efficacy of adjuvant CIK cell therapy

588 in epithelial ovarian cancer patients who received postoperative chemotherapy.
589 *Oncoimmunology* **8**, e1528411 (2019).
590 48. Barili, V. et al. Targeting p53 and histone methyltransferases restores exhausted
591 $CD8^+$ T cells in HCV infection. *Nat. Commun.* **11**, 604 (2020).
592
593 **Figure legend**
594 **Figure 1.** ARV-induced apoptosis in AGS cells through the TRAIL signaling pathway and
595 ARV-induced expression of TRAIL on PBMCs driven by IFN-γ sensitization. (A) AGS cells
596 were infected with ARV at an MOI of 10 for 24 h and sensitized in the presence or absence
597 of recombinant TRAIL protein (25 ng/mL). Sub-G1 cell populations were analyzed by flow
598 cytometry. Counts: the number of events (cell count) on the y-axis. (B) Graph shown
599 represents the mean± SE calculated from three independent experiments. *p<0. 05 * * p <
600 0.01. In this work, the statistical methods of Figures 2-8 are the same as the Fig. 1. (C)
601 AGS cells were infected with ARV at an MOI of 10 for 24 h and sensitized in the presence
602 or absence of recombinant TRAIL protein (25 ng/mL). Cell lysates were analyzed by
603 Western blot assays. All original/uncropped blots and images from this study are provided
604 in supplementary figure 7. (D) To detect cell death, annexin V and PI double staining was
605 used in flow cytofluorimetric analyses. The data generated by flow cytometry are plotted in
606 two-dimensional dot plots in which PI is represented versus annexin V-FITC. Apoptotic cells
607 which are PI and Annexin positive (PI/FITC +/+). PBMCs were sensitized with ARV at an
608 MOI of 10. TRAIL levels were analyzed 24 h post-sensitization. PBMCs were isolated from
609 normal healthy volunteers (n=3). Similar results were observed in 3 different PBMC samples.
610 The expression levels of TRAIL were examined by qRT-PCR (E) Western blot assays (F).
611 (G) TRAIL expression on human PBMC after ARV or UV-ARV sensitization. The
612 expression levels of TRAIL were analyzed by 24 h later on $CD3^+$, $CD14^+$, $CD19^+$, and

613 $CD56^+$ cells using two-color flow cytometry. Representative results are shown in histograms
614 based on 10^4 gated cells in all conditions, relative mean fluorescence intensity (RMFI) is
615 shown on histograms. Cell viability was >95%, as assessed by PI exclusion. Similar results
616 were observed using at least 3 different PBMC donors.
617
618 **Figure 2.** ARV-induced apoptosis in PGC cells through the TRAIL signaling. (A and
619 B) To confirm the normal epithelial cells, cytokeratin 18 (CK-18) staining was
620 performed. The highly positive staining for granulin (GRN) discriminated the PGC
621 cells from normal gastric cells. (C and D) PGC cells were infected with ARV at an MOI
622 of 10 for 24 h and sensitized in the presence or absence of recombinant TRAIL protein
623 (25 ng/mL). Sub-G1 cell populations were analyzed by flow cytometry. (E) To detect
624 cell death, annexin V/PI double staining was used in flow cytofluorimetric analyses.
625 The data generated by flow cytometry are plotted in two-dimensional dot plots in which
626 PI is represented versus annexin V-FITC. Apoptotic cells which are PI and annexin
627 positive (PI/FITC +/+). TRAIL expression on P-PBMCs after ARV and UV-ARV
628 sensitization. (F)The expression levels of TRAIL were analyzed 24 h later on $CD3^+$,
629 $CD14^+$, $CD19^+$, and $CD56^+$ cells using two-color flow cytometry, relative mean
630 fluorescence intensity (RMFI) is shown on histograms. Representative results are
631 shown in histograms based on 10^4 gated cells in all conditions, and cell viability was
632 >95%, as assessed by PI exclusion. Similar results were observed using at least 3
633 different P-PBMCs donors.
634
635 **Figure 3.** ARV or UV-ARV upregulates the IFN-γ expression levels in P-PBMCs. (A)
636 IFN-γ expression by P-PBMCs after ARV or UV-ARV stimulation. P-PBMCs were
637 sensitized with ARV or UV-ARV. Intracellular IFN-γ levels were analyzed 24 h post

638 treatment later in $CD3^+$ and $CD56^+$ cells using two-color flow cytometry. (B) P-PBMCs
639 cultured with 5 μg/ml anti-IFN-γ Ab or isotype control Ab for 1 h followed by
640 sensitization with ARV and cultured for 24 h. Representative results for $CD3^+$ and
641 $CD56^+$ cells are shown in histograms based on at least 10^4 gated cells. RMFI is shown
642 on histograms. Similar results were observed using 3 different P-PBMC donors. (C)
643 Decreasing numbers of P-PBMCs (ranging10^7to10^4) were stimulated with ARV or UV-
644 ARV, respectively. After stimulated, IFN-γ levels in the culture supernatants were
645 determined by ELISA.
646
647 **Figure 4.** ARV- and UV-ARV-sensitized P-PBMCs-dependent cytolysis of PGC cells
648 (PGCs). (A) P-PBMCs were co-cultured with PGCs followed by sensitization with
649 ARV for 24 h. The ratio of cell numbers of P-PBMCs (effector cells) and PGCs (target
650 cells) was 5:1. DR5:Fc (20 μg/ml) was used to inhibit ARV-sensitized P-PBMCs killing
651 PGCs. Fas:Fc (20 μg/ml) was used as a control negative. Cell death was measured by
652 SubG1 (A) and Annexin V/PI (B). Data represent the mean of triplicate experiments,
653 and experiments were repeated at least three times using different donor P-PBMCs with
654 similar results. (C) P-PBMCs were co-cultured with PGCs followed by sensitization
655 with ARV or UV-ARV for 24 h and 48 h, respectively. The ratio of coculture cell
656 numbers of P-PBMCs and PGCs was 5:1. Cell death was measured by LDH
657 cytotoxicity assay. Data represent the mean of triplicate experiments, and experiments
658 were repeated at three times using different donor P-PBMCs with similar results.
659
660 **Figure 5.** ARV or UV-ARV induces most immunogenic apoptosis in PGC cells (PGCs)
661 and upregulates the TRAIL expression levels by $CD8^+$TILs. (A) $CD8^+$T cells, $CD4^+$ T
662 cells, $CD56^+$NK cells, and $CD14^+$monocyte/macrophages were co-cultured with PGCs

663 followed by sensitization with ARV or UV-ARV for 24 h and 48 h, respectively. The
664 ratio of coculture cell numbers of TILs and PGCs was 5:1. Cell death was measured by
665 LDH cytotoxicity assay. Data represent the mean of triplicate experiments, and
666 experiments were repeated at three times using different donor TILs with similar results.
667 (B) The expression levels of TRAIL were analyzed on $CD8^+$ TILs 24 h post treatment
668 ARV or UV-ARV using two-color flow cytometry. Cell viability was >95%, as
669 assessed by PI exclusion. Similar results were observed using at least 3 different $CD8^+$
670 TILs donors. (C) $CD8^+$TILs cultured with 5 μg/ml anti-IFN-γ Ab or isotype control Ab
671 for 1 h, followed by sensitization with ARV or UV-ARV and cultured for 24 h.
672 Representative results for $CD8^+$ TILs are shown in histograms, RMFI is shown on
673 histograms. Similar results were observed using 3 different $CD8^+$ TILs donors.
674
675 **Figure 6.** ARV- or UV-ARV-sensitized $CD8^+$TILs expressing TRAIL which kills PGC
676 cells (PGCs). (A) $CD8^+$TILs were co-cultured with PGCs followed by sensitization
677 with ARV or UV-ARV for 24 h, respectively. The ratio of cell numbers of $CD8^+$TILs
678 (effector cells) and PGCs (target cells) was 5:1. DR5:Fc (20 μg/ml) was used to inhibit
679 ARV or UV-ARV-sensitized $CD8^+$TILs killing PGCs. Fas:Fc (20 μg/ml) was used as
680 a control negative. Cell death was measured by Sub-G1 (A), LDH cytotoxicity assay
681 (B), and Annexin V/PI (C). Similar results were observed using 3 different $CD8^+$TILs
682 donors. (D)PGCs were sensitized with UV-ARV (100 MOI) or ARV (10 MOI) for 24
683 h. Cell-surface DR4 and DR5 were analyzed by flow cytometry.
684
685 **Figure 7.** ARV σC and UV-ARV σC activate $CD8^+$ TILs through the TLR3/NF-κb/
686 IFN-γ pathway. ARV- or UV-ARV σC-interacted $CD8^+$ TILs release IFN-γ via the
687 TLR3-dependent NF-κB signaling pathway. (A) Proximity ligation assays for cell-

surface TLR3 on $CD8^+$ TILs. The interaction between ARV σC or UV-ARV σC and TLR3 ($CD8^+$ TILs) was assessed by PLA. Representative images are from three independent experiments. Cell nuclei were stained with DAPI (blue). (B-C) Analysis of IFN-γ production by ARV or UV-ARV sensitized-$CD8^+$TILs treated with TLR3 inhibitor or NF-κB inhibitor. $CD8^+$TILs were pretreated with or without TLR3 inhibitor (10 μg/mL) for 30 min and then sensitized with UV-ARV or ARV for 24 h. $CD8^+$TILs were incubated for 1 h with or without 10 μM BAY11-7082 and then sensitized with ARV or UV-ARV for 24 h. IFN-γ and $CD8^+$ was measured by flow cytometry.

Figure 8. The ARV or UV-ARV σC protein interacting with TLR3 of PGC cells and upregulation of DR4 and DR5 death receptors in ARV or UV-ARV-sensitized PGC cells through the p38/p53 signaling pathway. (A) Cell surface staining for DR4 and DR5 of PGC cells from patients was performed in cells pretreated with the p53 inhibitor for 5 h followed by treatment with ARV or UV-ARV. The working concentration for p53 inhibitor was 20 μM. Data are also presented as the ratio between MFI (Median fluorescence intensity) of patients. (B) Intracellular staining for p53 and p-p53(S15) of PGC cells treated ARV or UV-ARV were performed in presence of p38 inhibitor (20 μM). (C) p-p38 (T180) and p38 intracellular staining of PGC cells patients with or without TLR3 inhibitor (10 μg/mL) for 30 min followed by sensitization with UV-ARV or ARV for 24 h. (D) Proximity ligation assays for cell-surface TLR3 on PGC cells. The interaction between ARV σC or UV-ARV σC and TLR3 (PGC cells) was assessed by PLA. Representative images are from three independent experiments. Cell nuclei were stained with DAPI (blue).

Figure 9. Schematic diagram showing the ARV or UV-ARV-induced DR4/DR5

713 expression of PGC cells is dependent on σC-triggering the TLR3/P38/P53/DR4/DR5
714 pathway. ARV σC and UV-ARV σC activate $CD8^+$TILs to induce immunogenic
715 apoptosis through the TLR3/NF-κb/IFN-γ/TRAIL pathway. ARV σC and UV-ARV σC
716 activate $CD8^+$TILs to kill PGC cells.
717

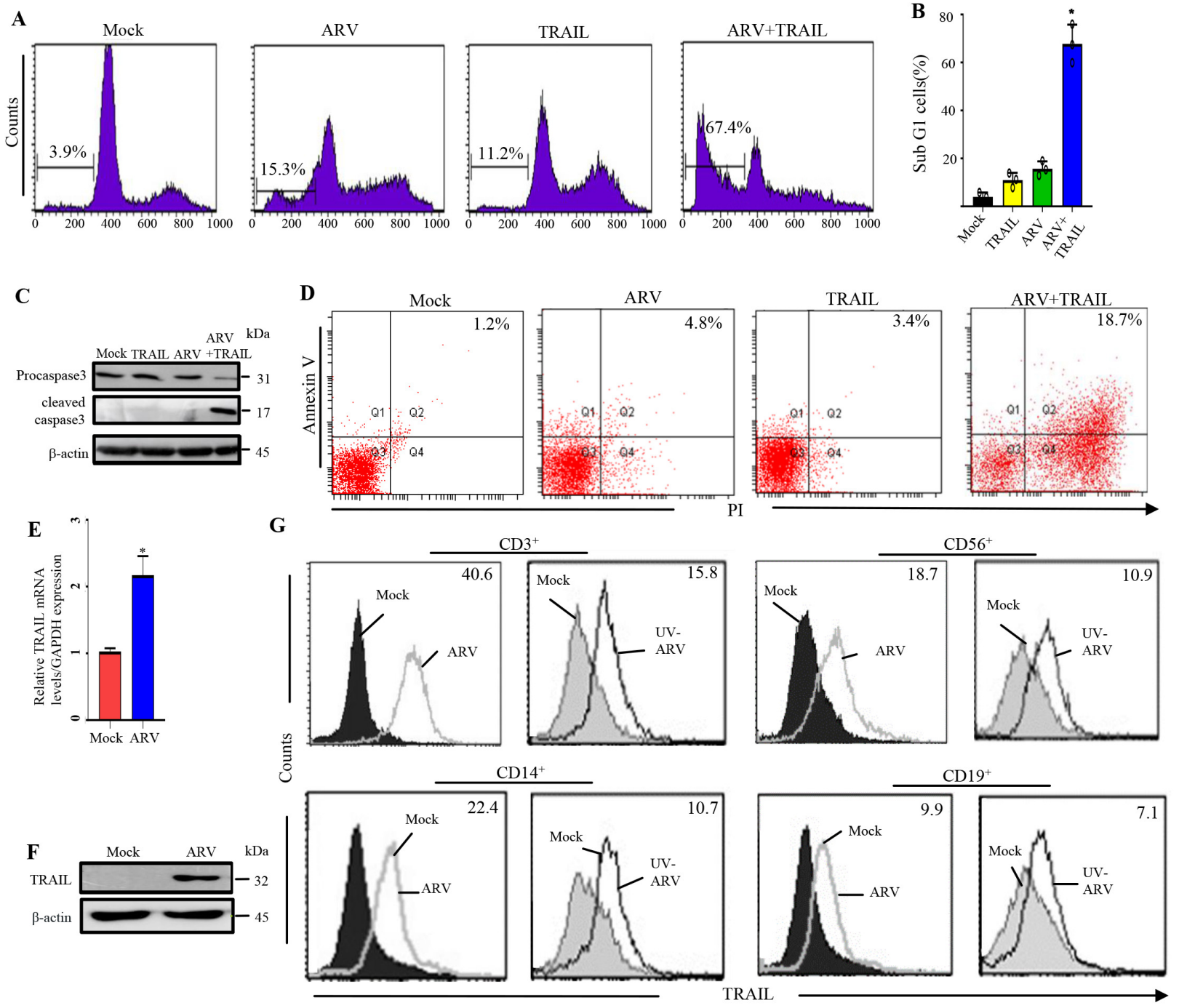
A
Mock
ARV
TRAIL
ARV+TRAIL
Counts
3.9%
15.3%
11.2%
67.4%
0
200
400
600
800
1000
B
Sub G1 cells(%)
80
60
40
20
Mock
TRAIL
ARV
ARV+ TRAIL
C
kDa
Mock TRAIL ARV ARV +TRAIL
Procaspase3
31
cleaved caspase3
17
β-actin
45
D
Mock
ARV
TRAIL
ARV+TRAIL
1.2%
4.8%
3.4%
18.7%
Annexin V
PI
Q1
Q2
Q3
Q4
E
Relative TRAIL mRNA levels/GAPDH expression
Mock
ARV
F
Mock
ARV
kDa
TRAIL
32
β-actin
45
G
CD3+
CD56+
CD14+
CD19+
40.6
15.8
18.7
10.9
22.4
10.7
9.9
7.1
Mock
ARV
UV-ARV
Counts
TRAIL

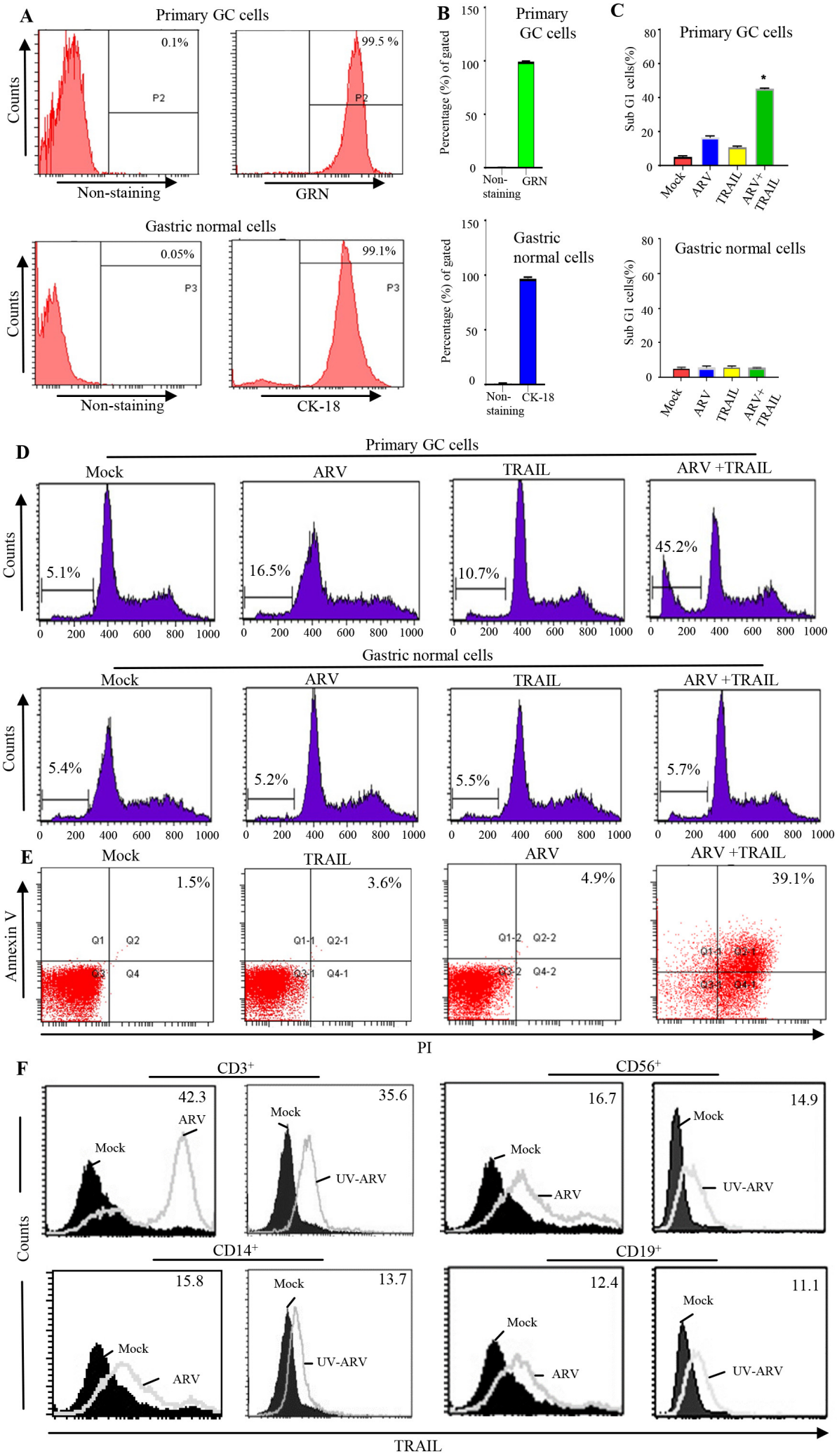
A
Primary GC cells
0.1%
P2
99.5 %
P2
Counts
Non-staining
GRN
Gastric normal cells
0.05%
P3
99.1%
P3
Counts
Non-staining
CK-18
B
Primary GC cells
Percentage (%) of gated
150
100
50
0
Non-staining
GRN
Gastric normal cells
Percentage (%) of gated
150
100
50
0
Non-staining
CK-18
C
Primary GC cells
Sub G1 cells(%)
80
60
40
20
0
*
Mock
ARV
TRAIL
ARV+ TRAIL
Gastric normal cells
Sub G1 cells(%)
80
60
40
20
0
Mock
ARV
TRAIL
ARV+ TRAIL
D
Primary GC cells
Mock
ARV
TRAIL
ARV +TRAIL
Counts
5.1%
16.5%
10.7%
45.2%
0 200 400 600 800 1000
Gastric normal cells
Mock
ARV
TRAIL
ARV +TRAIL
Counts
5.4%
5.2%
5.5%
5.7%
0 200 400 600 800 1000
E
Mock
TRAIL
ARV
ARV +TRAIL
Annexin V
1.5%
3.6%
4.9%
39.1%
Q1
Q2
Q4
Q1-1
Q2-1
Q4-1
Q1-2
Q2-2
Q4-2
PI
F
CD3+
42.3
ARV
Mock
35.6
Mock
UV-ARV
CD56+
16.7
Mock
ARV
14.9
Mock
UV-ARV
Counts
CD14+
15.8
Mock
ARV
13.7
Mock
UV-ARV
CD19+
12.4
Mock
ARV
11.1
Mock
UV-ARV
TRAIL

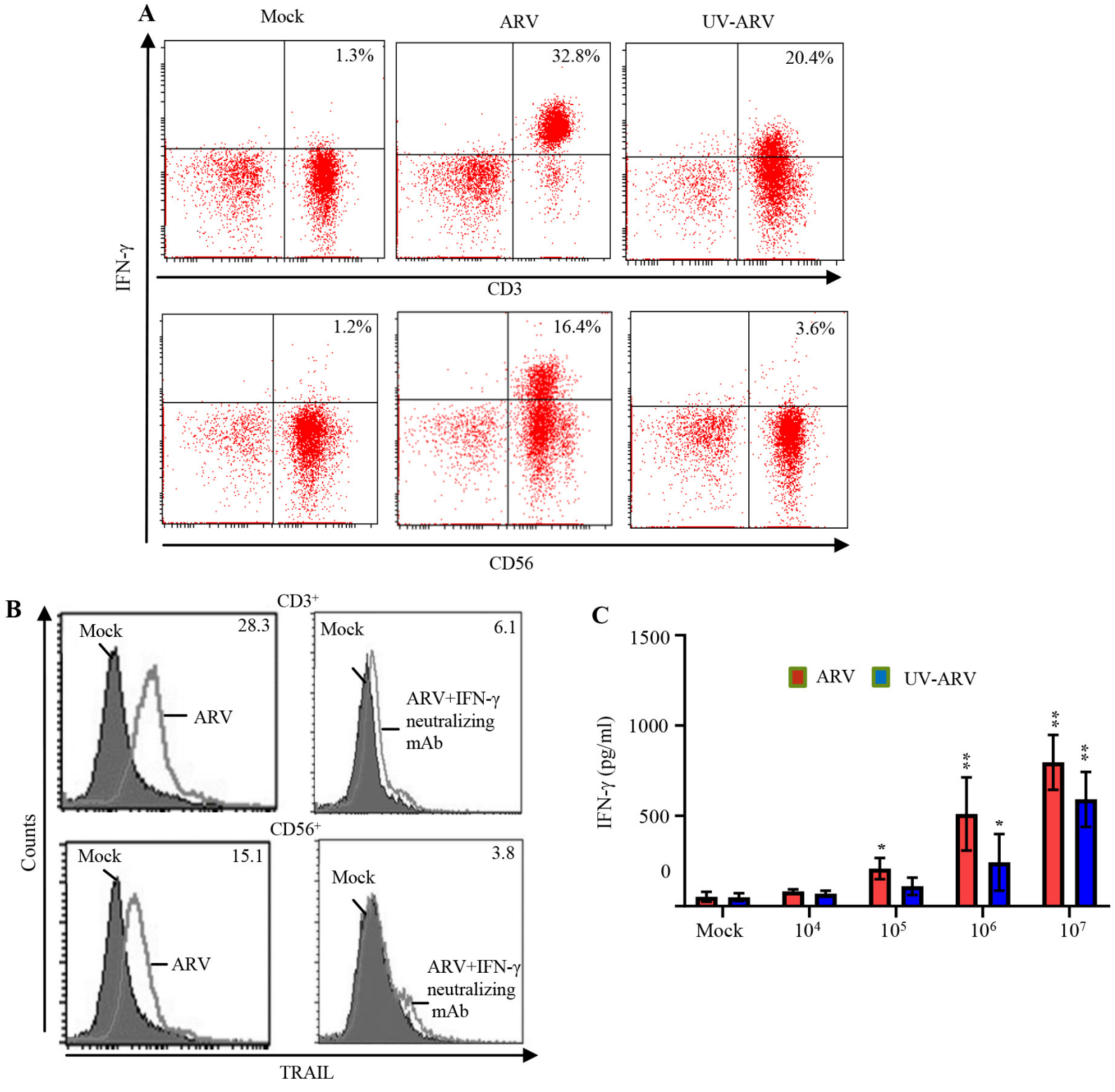
A
Mock
ARV
UV-ARV
1.3%
32.8%
20.4%
IFN-γ
CD3
1.2%
16.4%
3.6%
CD56
B
CD3+
Mock
28.3
ARV
Mock
6.1
ARV+IFN-γ neutralizing mAb
CD56+
Mock
15.1
ARV
Mock
3.8
ARV+IFN-γ neutralizing mAb
Counts
TRAIL
C
ARV
UV-ARV
IFN-γ (pg/ml)
1500
1000
500
0
Mock
10^4
10^5
10^6
10^7
*
**

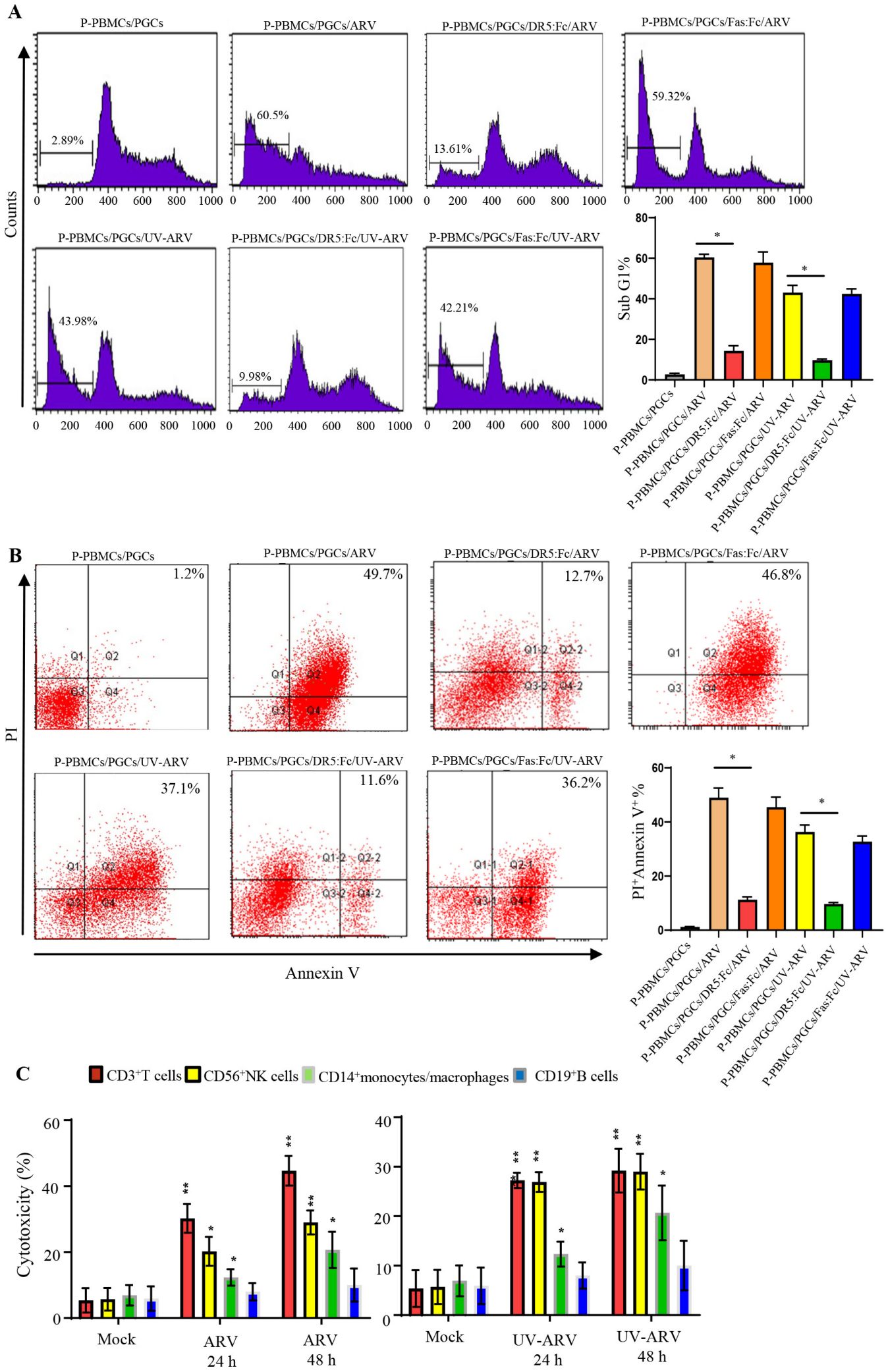
A
P-PBMCs/PGCs
P-PBMCs/PGCs/ARV
P-PBMCs/PGCs/DR5:Fc/ARV
P-PBMCs/PGCs/Fas:Fc/ARV
2.89%
60.5%
13.61%
59.32%
Counts
P-PBMCs/PGCs/UV-ARV
P-PBMCs/PGCs/DR5:Fc/UV-ARV
P-PBMCs/PGCs/Fas:Fc/UV-ARV
43.98%
9.98%
42.21%
0 200 400 600 800 1000
Sub G1%
0 20 40 60 80
*
*
P-PBMCs/PGCs
P-PBMCs/PGCs/ARV
P-PBMCs/PGCs/DR5:Fc/ARV
P-PBMCs/PGCs/Fas:Fc/ARV
P-PBMCs/PGCs/UV-ARV
P-PBMCs/PGCs/DR5:Fc/UV-ARV
P-PBMCs/PGCs/Fas:Fc/UV-ARV
B
P-PBMCs/PGCs
P-PBMCs/PGCs/ARV
P-PBMCs/PGCs/DR5:Fc/ARV
P-PBMCs/PGCs/Fas:Fc/ARV
1.2%
49.7%
12.7%
46.8%
Q1
Q2
Q3
Q4
Q1-2
Q2-2
Q3-2
Q4-2
PI
P-PBMCs/PGCs/UV-ARV
P-PBMCs/PGCs/DR5:Fc/UV-ARV
P-PBMCs/PGCs/Fas:Fc/UV-ARV
37.1%
11.6%
36.2%
Q1-1
Q2-1
Q3-1
Q4-1
Annexin V
PI+Annexin V+%
0 20 40 60
*
*
P-PBMCs/PGCs
P-PBMCs/PGCs/ARV
P-PBMCs/PGCs/DR5:Fc/ARV
P-PBMCs/PGCs/Fas:Fc/ARV
P-PBMCs/PGCs/UV-ARV
P-PBMCs/PGCs/DR5:Fc/UV-ARV
P-PBMCs/PGCs/Fas:Fc/UV-ARV
C
CD3+T cells
CD56+NK cells
CD14+monocytes/macrophages
CD19+B cells
Cytotoxicity (%)
0 20 40 60
0 10 20 30 40
**
*
Mock
ARV 24 h
ARV 48 h
UV-ARV 24 h
UV-ARV 48 h

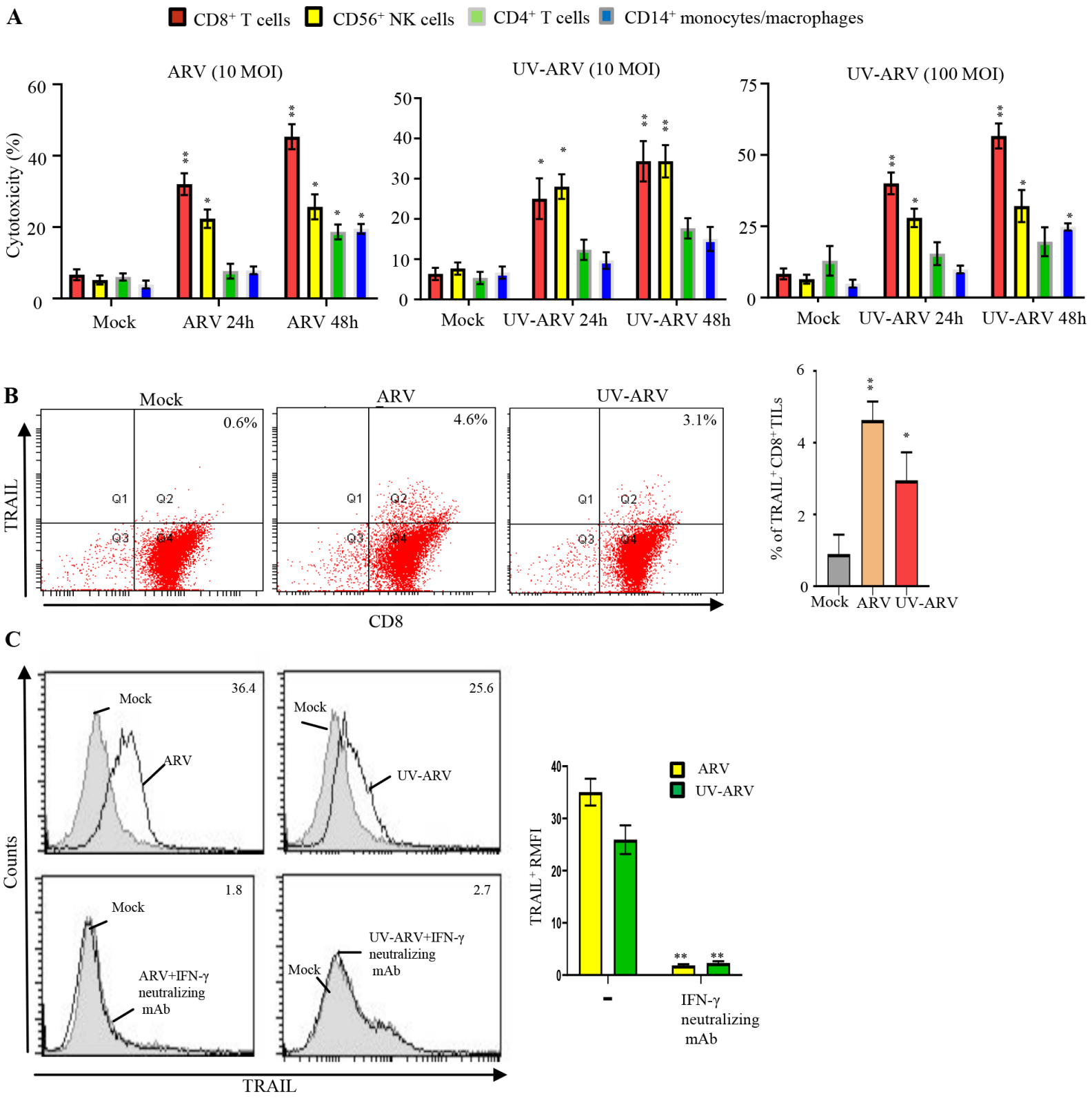
A
CD8+ T cells
CD56+ NK cells
CD4+ T cells
CD14+ monocytes/macrophages
ARV (10 MOI)
UV-ARV (10 MOI)
UV-ARV (100 MOI)
Cytotoxicity (%)
Mock
ARV 24h
ARV 48h
UV-ARV 24h
UV-ARV 48h
B
Mock
ARV
UV-ARV
0.6%
4.6%
3.1%
Q1
Q2
Q3
Q4
TRAIL
CD8
% of TRAIL+CD8+TILs
C
36.4
25.6
1.8
2.7
Mock
ARV
UV-ARV
ARV+IFN-γ neutralizing mAb
UV-ARV+IFN-γ neutralizing mAb
Counts
TRAIL
TRAIL+ RMFI
IFN-γ neutralizing mAb

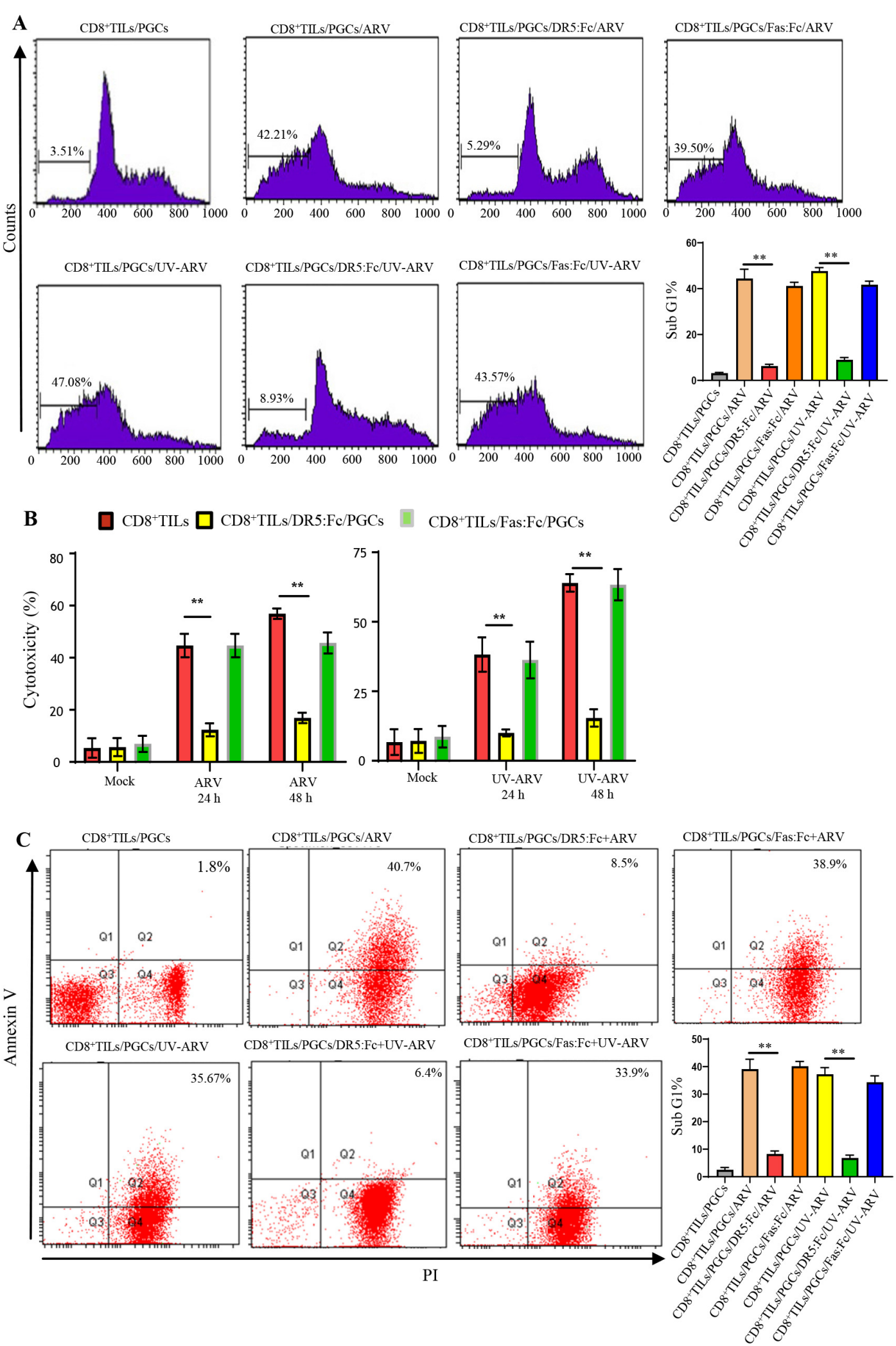
A
CD8+TILs/PGCs
CD8+TILs/PGCs/ARV
CD8+TILs/PGCs/DR5:Fc/ARV
CD8+TILs/PGCs/Fas:Fc/ARV
CD8+TILs/PGCs/UV-ARV
CD8+TILs/PGCs/DR5:Fc/UV-ARV
CD8+TILs/PGCs/Fas:Fc/UV-ARV
3.51%
42.21%
5.29%
39.50%
47.08%
8.93%
43.57%
Counts
Sub G1%
B
CD8+TILs
CD8+TILs/DR5:Fc/PGCs
CD8+TILs/Fas:Fc/PGCs
Cytotoxicity (%)
Mock
ARV 24 h
ARV 48 h
UV-ARV 24 h
UV-ARV 48 h
C
1.8%
40.7%
8.5%
38.9%
35.67%
6.4%
33.9%
Q1
Q2
Q3
Q4
Annexin V
PI
Sub G1%

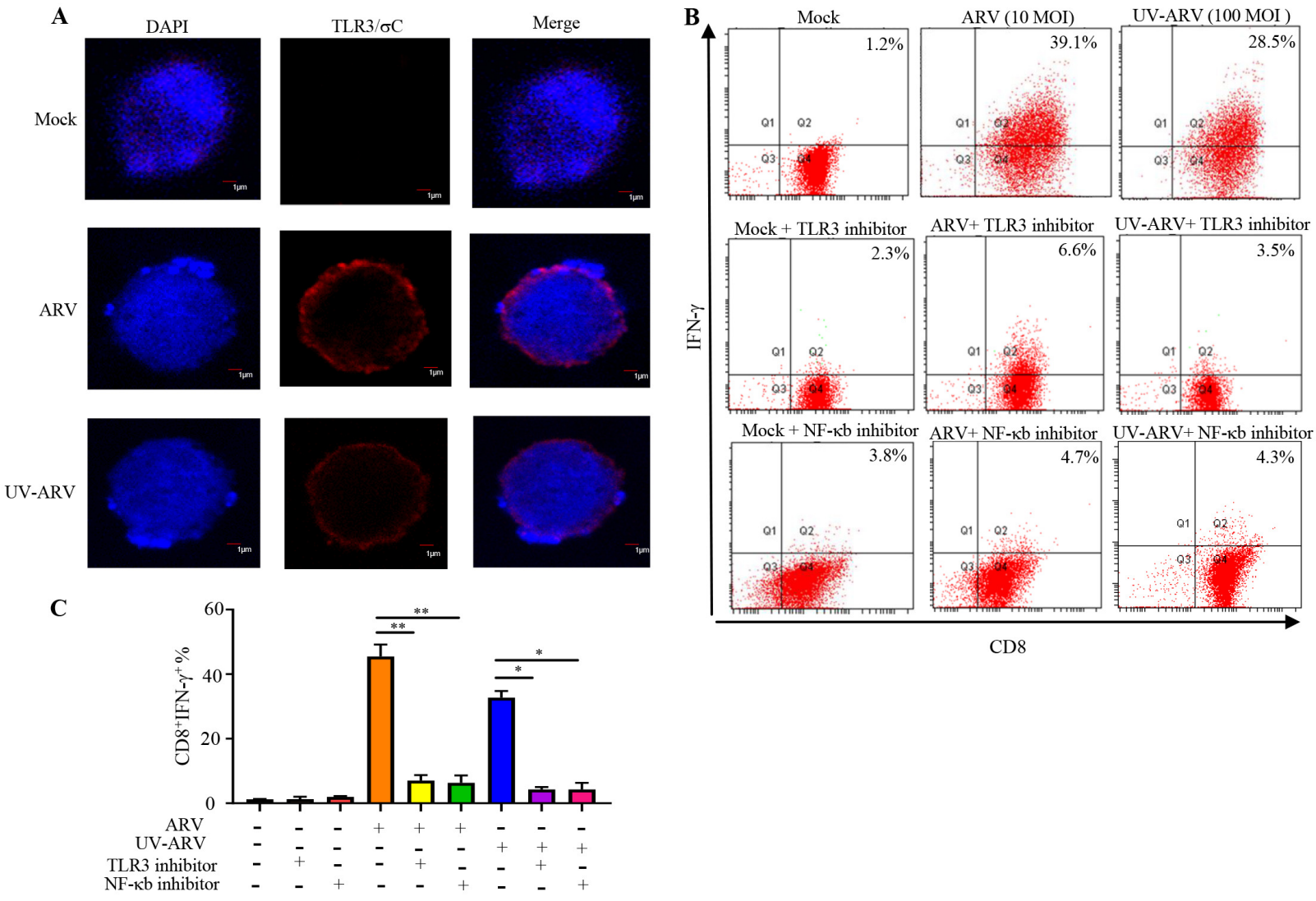
A
DAPI
TLR3/σC
Merge
Mock
ARV
UV-ARV
1μm
B
Mock
ARV (10 MOI)
UV-ARV (100 MOI)
1.2%
39.1%
28.5%
Mock + TLR3 inhibitor
ARV+ TLR3 inhibitor
UV-ARV+ TLR3 inhibitor
2.3%
6.6%
3.5%
Mock + NF-κb inhibitor
ARV+ NF-κb inhibitor
UV-ARV+ NF-κb inhibitor
3.8%
4.7%
4.3%
Q1
Q2
Q3
Q4
IFN-γ
CD8
C
CD8+IFN-γ+ %
60
40
20
0
**
**
*
*
ARV
UV-ARV
TLR3 inhibitor
NF-κb inhibitor

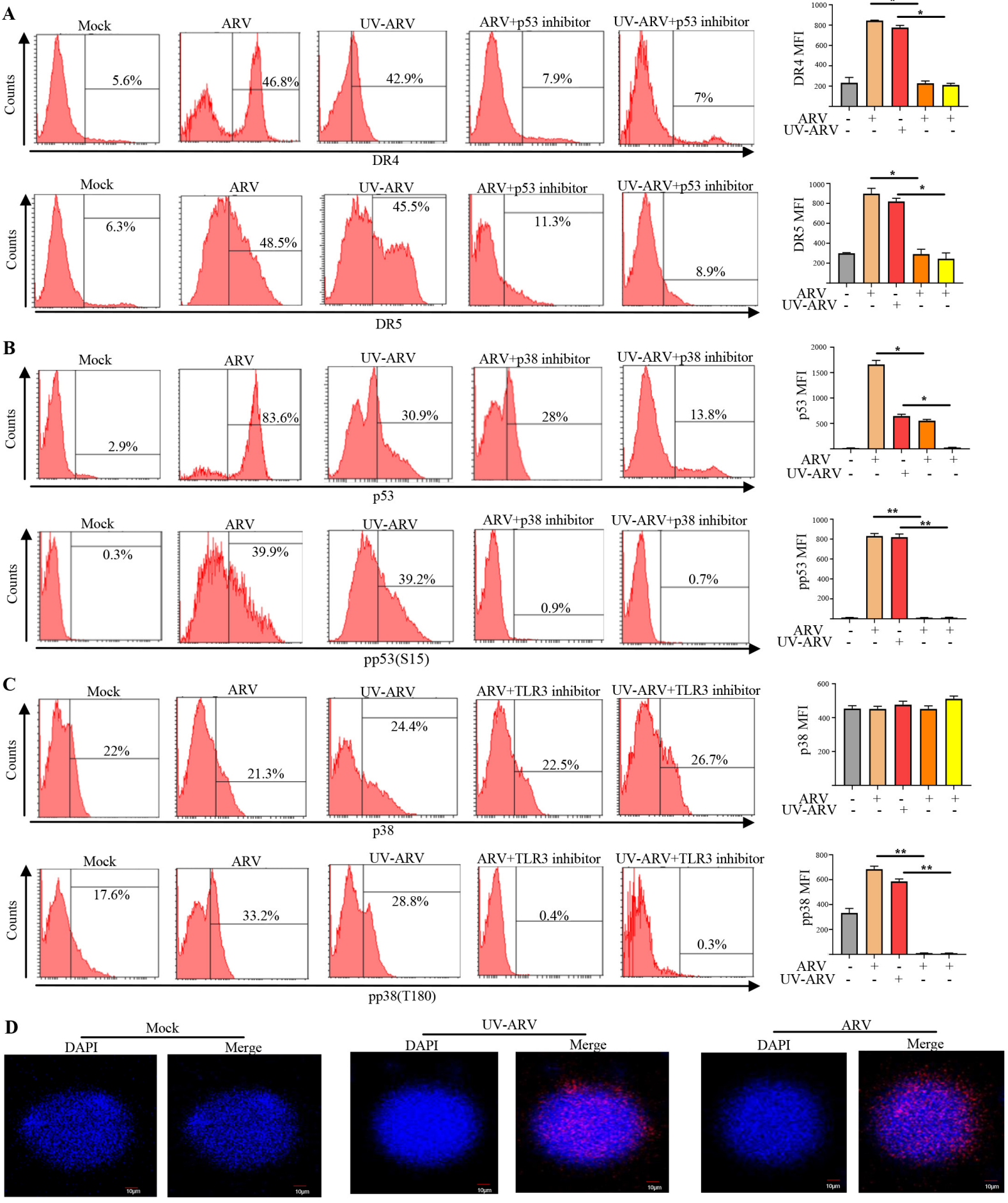
A
Mock
ARV
UV-ARV
ARV+p53 inhibitor
UV-ARV+p53 inhibitor
Counts
5.6%
46.8%
42.9%
7.9%
7%
DR4
DR4 MFI
ARV
UV-ARV
6.3%
48.5%
45.5%
11.3%
8.9%
DR5
DR5 MFI
B
ARV+p38 inhibitor
UV-ARV+p38 inhibitor
2.9%
83.6%
30.9%
28%
13.8%
p53
p53 MFI
0.3%
39.9%
39.2%
0.9%
0.7%
pp53(S15)
pp53 MFI
C
ARV+TLR3 inhibitor
UV-ARV+TLR3 inhibitor
22%
21.3%
24.4%
22.5%
26.7%
p38
p38 MFI
17.6%
33.2%
28.8%
0.4%
0.3%
pp38(T180)
pp38 MFI
D
DAPI
Merge
10μm

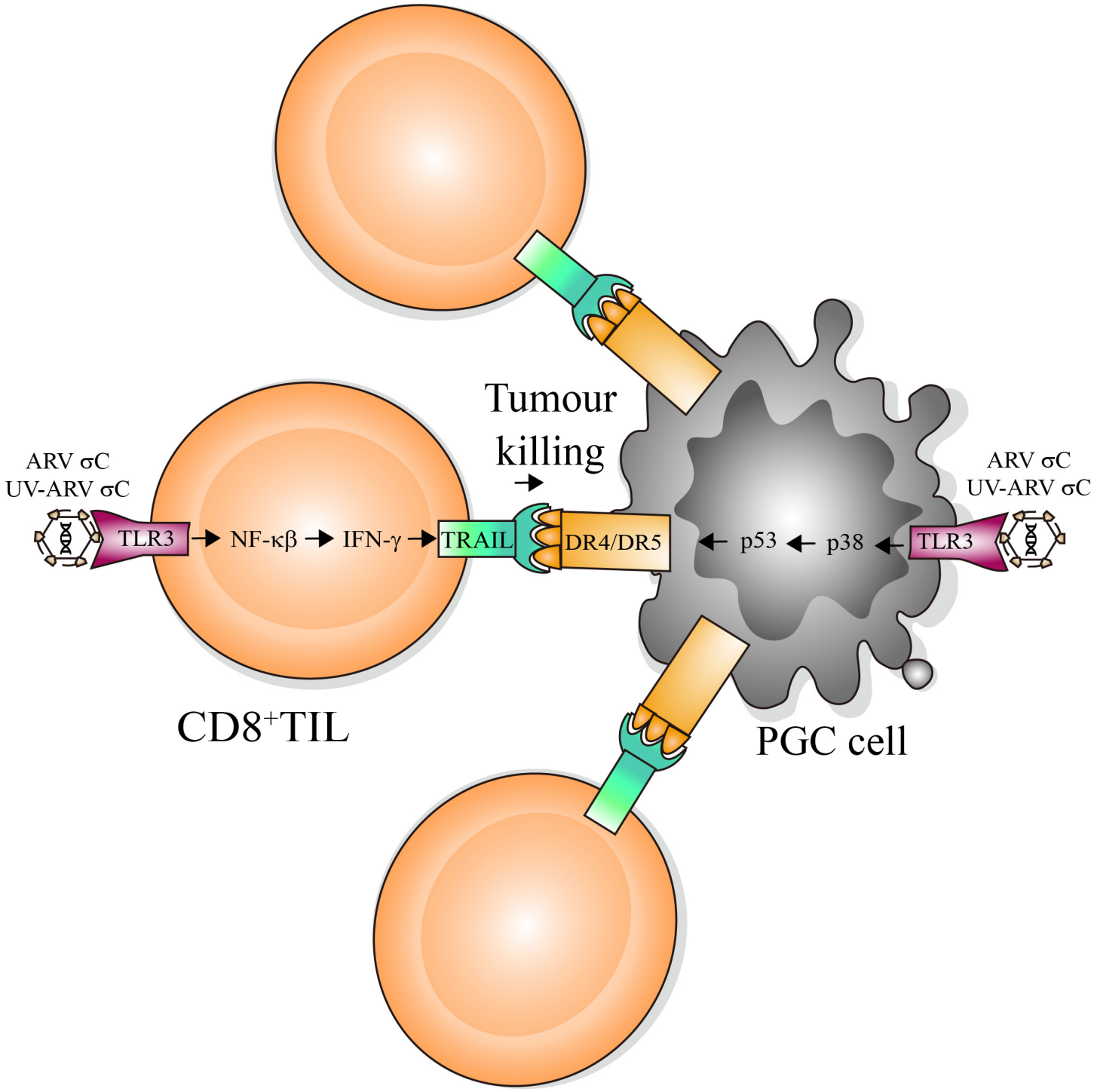
Tumour killing
ARV σC
UV-ARV σC
TLR3
NF-κβ
IFN-γ
TRAIL
DR4/DR5
p53
p38
TLR3
ARV σC
UV-ARV σC
CD8+TIL
PGC cell

Table1 Clinical characteristics of each sample used in this study

Pt	Age	Gender	Histopathological diagnosis	Site of origin	Lauren's classification	Helicobacter pylori
1	60s	F	Poorly differentiated adenocarcinoma	Antrum	Diffuse	Positive
2	50s	M	Moderately to poorly differentiated adenocarcinoma	Greater curvture	Mixed	Negative
3	70s	F	Moderately differentiated adenocarcinoma	Angular incisure	Instestinal	Negative
4	40s	M	Moderately to poorly differentiated adenocarcinoma	Antrum	Instestinal	Negative
5	60s	F	Moderately differentiated adenocarcinoma	Angular incisure	Instestinal	Positive
6	60s	M	Poorly differentiated adenocarcinoma	Greater curvture	Instestinal	Negative
7	50s	F	Poorly differentiated adenocarcinoma	Body	Diffuse	Negative
8	60s	M	Poorly differentiated adenocarcinoma	Lesser curvture	Diffuse	Negative
9	40s	F	Moderately differentiated adenocarcinoma	Lesser curvture	Instestinal	Negative
10	50s	M	Poorly differentiated adenocarcinoma	Greater curvture	Diffuse	Negative
11	50s	M	Enteroblastic differentiation	Lesser curvture	Not defined	N/A
12	50s	F	Poorly differentiated adenocarcinoma	Antrum	Diffuse	Negative
13	60s	M	Moderately differentiated adenocarcinoma	Antrum	Instestinal	Negative
14	60s	M	Poorly differentiated	Cardiac	Diffuse	Negative
15	70s	F	Moderately differentiated adenocarcinoma	Cardia	Instestinal	Negative
16	60s	F	Moderately differentiated adenocarcinoma	Lesser curvture	Intestinal	Negative
17	70s	M	Moderately to poorly differentiated adenocarcinoma	Antrum	Intestinal	Positive
18	60s	M	Poorly differentialted adenocarcinoma	Angular incisure	Diffuse（or mixed）	Negative
19	50s	M	Moderately differentiated adenocarcinoma	Antrum	Diffuse	Positive
20	70s	M	Moderately to poorly differentiated	Cardia	Diffuse	Negative

			adenocarcinoma			
21	40s	F	Moderately differentiated adenocarcinoma	Cardia	Intestinal	Negative

Pt: Patient; Helicobacter pylori: Histological identification

N/A: not available